CrossMark

ORIGINAL PAPER

Continuous in situ monitoring of sediment deposition in shallow benthic environments

James Whinney[1,4] · Ross Jones[2,3,4] · Alan Duckworth[2,3,4] · Peter Ridd[1,4]

Abstract Sedimentation is considered the most widespread contemporary, human-induced perturbation on reefs, and yet if the problems associated with its estimation using sediment traps are recognized, there have been few reliable measurements made over time frames relevant to the local organisms. This study describes the design, calibration and testing of an in situ optical backscatter sediment deposition sensor capable of measuring sedimentation over intervals of a few hours. The instrument has been reconfigured from an earlier version to include 15 measurement points instead of one, and to have a more rugose measuring surface with a microtopography similar to a coral. Laboratory tests of the instrument with different sediment types, colours, particle sizes and under different flow regimes gave similar accumulation estimates to SedPods, but lower estimates than sediment traps. At higher flow rates ($9\text{–}17$ cm s^{-1}), the deposition sensor and SedPods gave estimates $>10\times$ lower than trap accumulation rates. The instrument was deployed for 39 d in a highly turbid inshore area in the Great Barrier Reef. Sediment deposition varied by several orders of magnitude, occurring in either a relatively uniform (constant) pattern or a pulsed pattern characterized by short-term (4–6 h) periods of 'enhanced' deposition, occurring daily or twice daily and modulated by the tidal phase. For the whole deployment, which included several very high wind events and suspended sediment concentrations (SSCs) >100 mg L^{-1}, deposition rates averaged 19 ± 16 mg cm^{-2} d^{-1}. For the first half of the deployment, where SSCs varied from <1 to 28 mg L^{-1} which is more typical for the study area, the deposition rate averaged only 8 ± 5 mg cm^{-2} d^{-1}. The capacity to measure sedimentation rates over a few hours is discussed in terms of examining the risk from sediment deposition associated with catchment run-off, natural wind/wave events and dredging activities.

Keywords Sedimentation · Turbidity · Coral reefs · Sediment trap · Deposition sensor

✉ James Whinney
james.whinney@jcu.edu.au

Ross Jones
r.jones@aims.gov.au

1 Intelligent Systems, Information and Modelling, College of Science, Technology and Engineering, Townsville, QLD, Australia

2 Australian Institute of Marine Science, Perth, WA, Australia

3 Australian Institute of Marine Science, Townsville, QLD, Australia

4 Western Australian Marine Science Institution, Perth, WA, Australia

Introduction

In shallow benthic environments sediments can be temporarily released into the water column by natural wind and wave events, river plumes from catchment run-off, and dredging and dredging-related activities. The suspended sediments can have a range of effects on filter-feeders and, by changing the quantity and quality of light, on photoautotrophs such as corals and seagrasses (Rogers 1990; Anthony and Connolly 2004; Anthony et al. 2004; Erftemeijer and Lewis 2006; Foster et al. 2010; Jones et al. 2016). The sediments can also subsequently fall out of suspension, increasing sedimentation rates and making benthic organisms expend energy self-cleaning. Many studies have highlighted the significance of sedimentation on coral reefs (reviewed by Rogers 1990; Jones et al. 2016), and sedimentation is '…considered one of the most

🖄 Springer

widespread contemporary, human-induced perturbations on reefs…' (ISRS 2004).

Understanding the environmental risk associated with suspended sediments and sediment deposition is predicated on establishing a relationship between physical and chemical changes in the water column and the response of the underlying communities. Some of the physical changes are comparatively simple to measure, such as benthic light availability which can be routinely measured with submersible photosynthetically active radiation (PAR) quantum light sensors. Suspended sediment concentrations (SSCs) and turbidity can be highly correlated, and there are many commercially available optical devices (nephelometers) for recording turbidity (Gray and Gartner 2009, 2010). Sediment deposition, however, has proven difficult to measure at scales which are relevant to the physiology of local organisms (mg cm^{-2} d^{-1}, see review by Thomas and Ridd 2004). This is unfortunate, as at least for dredging, increased sedimentation and smothering is one of the key causal pathways leading to mortality of marine organisms in the short term (Jones et al. 2016).

In the absence of suitable techniques for sediment deposition monitoring, sediment traps have routinely been used to estimate sedimentation rates. Because of their simple design (open-ended tubes) and construction (e.g. PVC pipes) they have frequently been used for describing sedimentation rates on reefs (English et al. 1997; Storlazzi et al. 2011; Browne et al. 2012). However, there are many problems associated with using sediment traps to quantify the vertical flux of material in shallow energetic environments that are typical of coral reef environments (Wolanski 1994; Larcombe et al. 1995; Ogston et al. 2004; Storlazzi et al. 2011). These problems have been discussed many times in many different marine environmental settings (Hargrave and Burns 1979; Reynolds et al. 1980; Butman et al. 1986; Kozerski 1994; Jürg 1996; Buesseler et al. 2007), including coral reefs (Ridd et al. 2001; Thomas and Ridd 2004; Bothner et al. 2006; Risk and Edinger 2011; Storlazzi et al. 2011; Browne et al. 2012; Jones et al. 2016). Essentially, sediments entering traps have a lower chance of resuspension than sediment settling on the adjacent seabed, and traps therefore provide an estimate of gross rather than net sedimentation rate (see Cortes and Risk 1985). Sediment traps can also favour deposition due to hydrodynamic disturbance of the flow around the trap.

Recently, sediment pods (SedPods) have been suggested as an alternative technique for estimating sedimentation in situ. These are concrete-filled PVC hubs which act as a proxy for a flat, encrusting coral surface. Because they do not suffer the resuspension limitation and deposition bias of traps, they can provide better estimates of net rather than gross sedimentation (Field et al. 2012). Notwithstanding the issue of what sediment traps actually measure (see Storlazzi et al. 2011), another significant problem is that

they have to be left in situ for extended periods (days to weeks), and accumulation rates estimated by averaging over the deployment period. This provides at best a very coarse assessment of temporal patterns of sediment deposition. The same issue applies for SedPods.

For more realistic estimates of sediment deposition, and over much shorter timescales, one of the more promising techniques is a deposition sensor based on optical backscatter sensor (OBS) principles (Ridd et al. 2001; Thomas and Ridd 2005). The instrument uses fibre optic bundles set into a horizontal measuring surface and connected to an infra-red LED and a light sensor. The amount of light from the LED that is back-scattered into the sensor varies in proportion to the amount of sediment that has settled (Ridd et al. 2001; Thomas et al. 2003a, b; Thomas and Ridd 2005). Some of the known limitations of the deposition sensor are that measurements are made at a single point, and that the flat deposition plate is very smooth, sometimes resulting in rapid resuspension and even saltation of sediments across the surface, giving low or sometimes spurious readings.

To address some of these issues, the deposition sensor has recently been redesigned to increase the number of sensors and to incorporate a more standardized measuring surface. Since net sediment deposition is dependent on the surface, a surface that more closely approximated the complex and typically rugose microtopography of a coral surface was selected. As with the use of the OBS principle for surrogate (proxy) monitoring of SSCs, differences in number, size, colour, density and shape of suspended particles, and refractive index (the light-scattering properties) need to be considered (Baker and Lavelle 1984; Conner and De Visser 1992; Gibbs and Wolanski 1992; Thackston and Palermo 2000; Gray and Gartner 2010; Storlazzi et al. 2015).

In this study, we describe the redesign of the deposition sensor, and its calibration and laboratory testing in response to different sediment types and different flow regimes. We also report on field deployment of the sensor in a highly turbid, inshore reef community of the central Great Barrier Reef (GBR). The deployment included calm, benign periods and storm periods. The study reports previously undescribed sub-daily patterns of sediment deposition providing new insights into absolute and relative patterns of one of the key anthropogenic 'pollutants' on coral reefs.

Materials and methods

All laboratory testing was conducted at the Australian Institute of Marine Science (AIMS) Sea Simulator (SeaSim) at Cape Cleveland and field work was conducted at Middle Reef in Cleveland Bay, in the turbid inner shelf reef zone of the central GBR (Fig. 1).
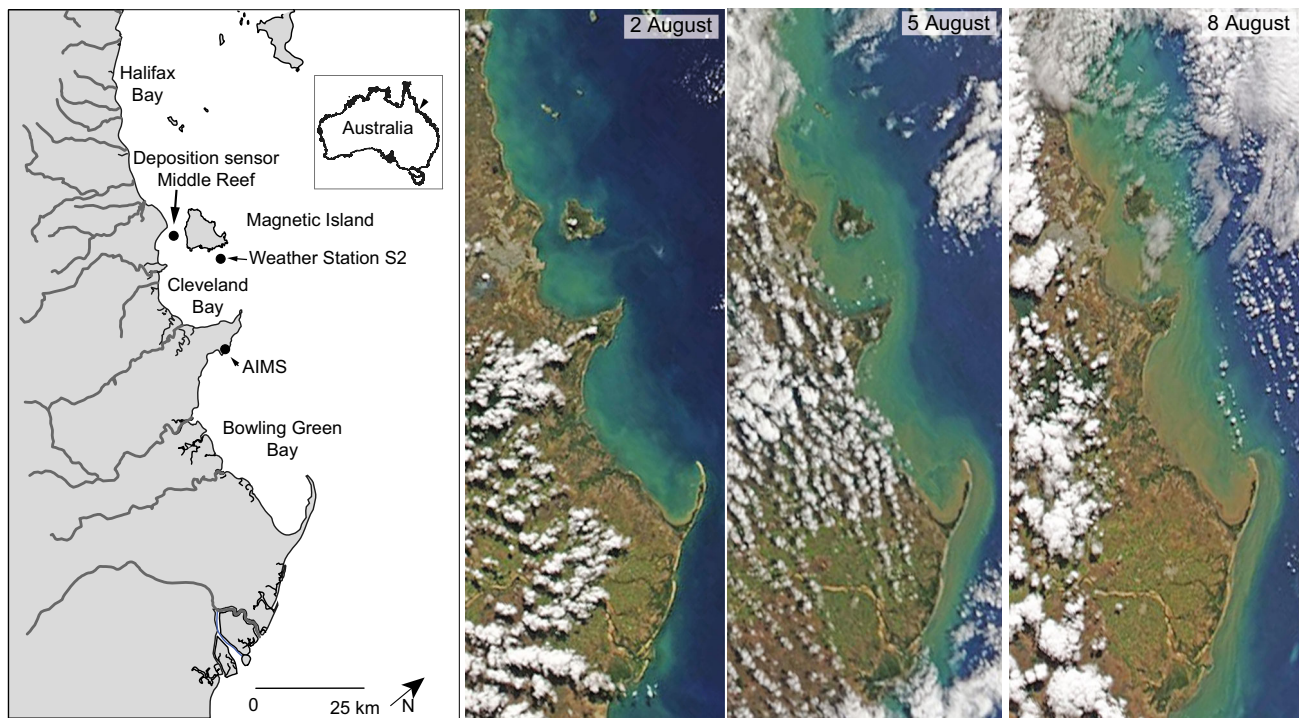
Fig. 1 Location map showing the deposition sensor deployment site (19°11.776′S, 146°8.886′E°) at Middle Reef in Cleveland Bay (central, inshore Great Barrier Reef region) and Moderate Resolution Imaging Spectroradiometer (MODIS) images of the study area on 2, 5 and 8 August 2014

The sediment deposition sensor was tested in a series of laboratory experiments where high SSCs were created and allowed to settle onto the deposition sensor and nearby SedPods and sediment traps. Tests were conducted with different sediment types, colours and particle size distributions (PSDs) and conducted under no flow (static) conditions and different flow regimes. Sediments for the laboratory studies were collected from 5 to 9 m depth by Smith-McIntyre grab or by scuba divers from three different coastal reef settings in Australia. Sediment types were (1) light grey predominantly carbonate (biogenic) sediment from the central GBR (Davies Reef, 18°49.507′S, 147°38.826′E), (2) yellow-brown mixed terrigenous mud and carbonate sediment collected at Middle Reef (Cleveland Bay, 19°11.722′S, 146°48.822′E), or (3) red-brown predominantly siliciclastic sediment collected from the nearshore region of north-west Australia (Pilbara region, 21°37.940′S, 115°0.175′E). All sediments were screened to 2 mm and then ground with a rod mill grinder until the mean grain size was ∼30 μm (range 0.5–140 μm) as measured using laser diffraction techniques (Mastersizer 2000, Malvern instruments Ltd, UK). A portion of the sediments of each type were then passed through a series of industrial sieves to create finer PSDs where necessary.

Measurement principle and sensor calibration

The newly designed instrument now has three separate sensor blocks arranged in a triangular pattern with each block embedded with five bundles of fibre optics which terminate on the sensor block (Fig. 2). The fibre optics from all five bundles in each block are connected to a single infra-red LED and optical sensor, so the 15 separate fibre optic bundles produce three separate measurements, each an average of five bundles. Overlying the sensor platform is a 170 × 3 mm head plate made of copper (to prevent biofouling for field studies), or acetal homopolymer resin (Delrin) for laboratory studies in confined aquaria. The 3-mm-thick plate is perforated with hundreds of equally distributed, countersunk apertures, and the size and spacing between the apertures is designed to mimic the calices of a coral. The measuring surface is designed to be a topographically complex, rugose surface that more closely approximates a generic encrusting coral with evenly spaced, medium-sized corallites than the previous smooth (glassy) measuring surface. The design principles are further expanded upon in the Discussion. Sediment depositing on the head plate falls through the apertures allowing optical measurement of sediment accumulation from those apertures that sit over an underlying fibre optic bundle (see
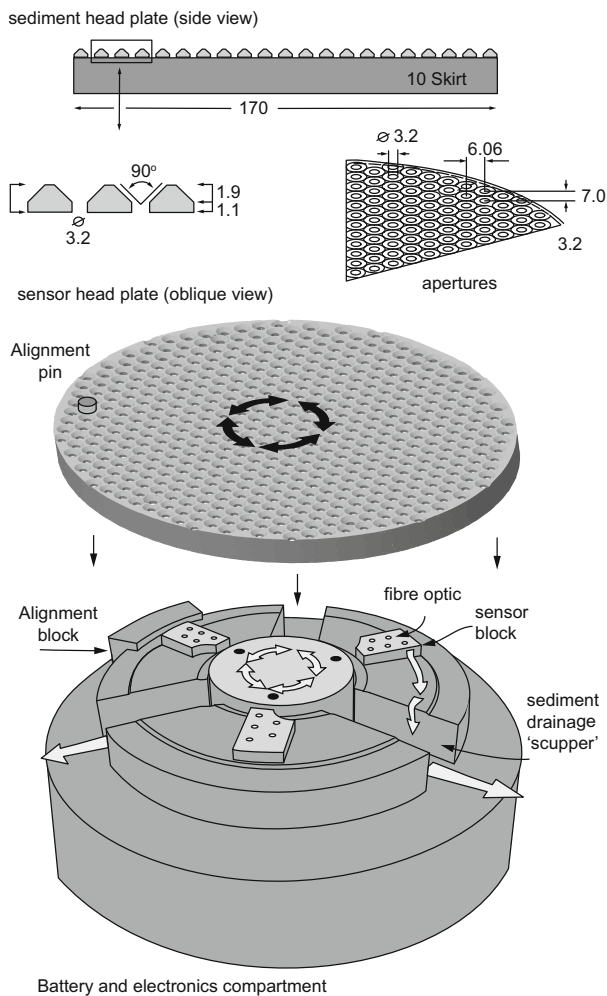
Fig. 2 Deposition sensor showing side and oblique views of the newly designed sensor head plate (see text for details). All length measurements are in mm

Fig. 2). Every hour the sensor head plate rotates 30° backwards and forwards several times to shift sediments that have accumulated on the fibre optics. Sediment passing through the head plate eventually exits through scuppers on the side of the instrument. The final rotation of the sensor head ends when an alignment pin comes into contact with an alignment block, which results in the centre of some of the apertures aligning to the centre of the fibre optic bundle. The sensor measures backscatter every 10 min, and changes in these readings provide an assessment of sedimentation rate. Periodic wiping, typically every 1–2 h, prevents sediment build-up from exceeding the measurement range of the sensor, and the interval between wipes is selected depending on the local sedimentary setting.

Calibration involves relating the mV signals from the backscatter sensor to mass per unit area (mg cm^{-2}) using sediment-specific conversion factors to account for differences in the sediment light-scattering properties. Calibrations were performed in a 3-m perspex settling tube, with

sediment introduced to the top of the tube and allowed to settle on a plate suspended from a mass balance 5 mm above the sensor plate surface. The weight of the sediment on the balance is converted from a weight in water into mass using the relative densities of water and the sediment. The total mass of sediment is divided by the surface area of the plate to give a mg cm^{-2} sediment mass surface density which was compared to the instrument readings.

Laboratory tests

All experiments were conducted in a 1200-L fibreglass tank using 0.4-μm-filtered seawater at salinity of 33 PSU and temperature of 27 °C. At the start of the experiments the sediments were mixed with 2 L of 0.4-μm-filtered seawater in a domestic blender for 2 min to create sediment slurry which was then added to the tanks and mixed thoroughly using submersible pumps. A range of sedimentation rates was generated by creating different SSCs (range 10–800 mg L^{-1}) and turning the pumps off to allow the sediments to gradually settle out of suspension. For experiments examining deposition under different flow rates, the submersible pumps were operated under different power levels to produce variable flow as measured by an acoustic Doppler velocimeter (16-MHz MicroADV, SonTek, CA, USA).

During the studies the deposition sensor was mounted on a perforated fibreglass grid floor, with the sensor head platform located 50 cm below the water surface. Five PVC sediment traps with an aspect ratio of 6:1 and a mouth surface area of 2.4 cm^2, and five PVC SedPods with a surface area of 25.2 cm^2 were placed beside the deposition sensor. At the end the experiments the sediment traps and SedPods were capped, and any trapped or accumulated sediment determined gravimetrically. Sediment samples were filtered through pre-weighed 0.4-μm, 47-mm-diameter polycarbonate filters, incubated at 60 °C for ≥24 h and weighed to determine sediment mass.

Field tests

The deposition sensor was deployed at 5–6 m depth in the inshore turbid reef systems of the central GBR (Fig. 1) from 14 July to 22 August 2014. The sensor recorded measurements ∼30 cm from the seafloor, ∼2–3 m from Middle Reef, and was programmed to self-clean every 1 h. The sensor was deployed beside an instrument platform which included a sideways-mounted nephelometer, upwards-facing 2π quantum PAR sensor, water temperature sensor and a pressure sensor (Macdonald et al. 2013). Each sensor reading is an average of 250 measurements over a 1-s period. All sensors take one reading every 10 min except for the pressure sensor which takes ten consecutive readings. Water pressure readings were converted to water depth using the hydrostatic equation and the
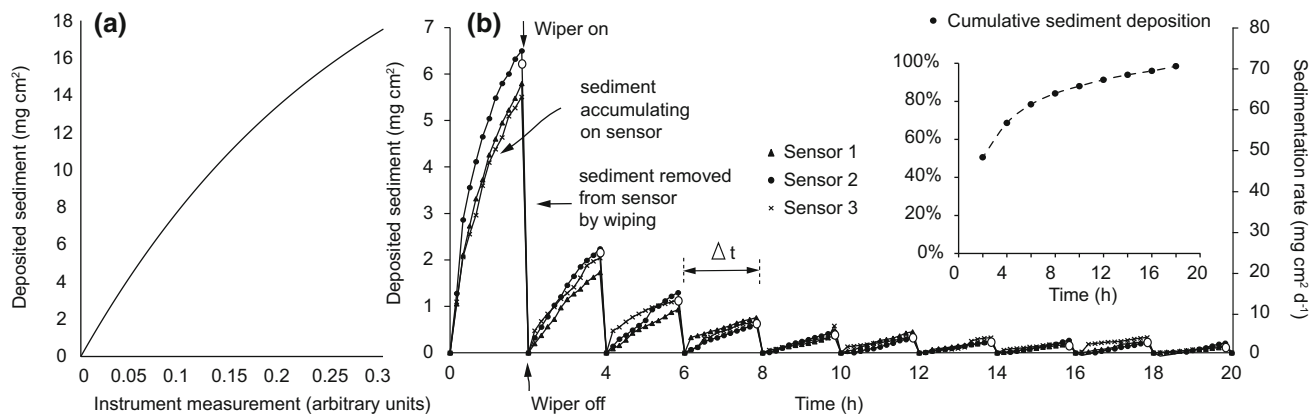
Fig. 3 An example of the pattern of sediment deposition in a static, laboratory-based study using very finely ground, light grey, carbonate sediments with a mean particle size 6.4 μm (with 95% of the particles <20 μm), showing **a** instrument calibration whereby sediment depositing on the surface of the fibre optics is converted to mass (mg) per unit area (cm^2) and **b** the saw-tooth pattern generated by cleaning of the fibre optics by the wiper mechanism (every 2 h). The *inset* shows the cumulative sediment deposition, indicating that >50% of the sediment settled out in the first 2 h of the experiment (see text for further details)

root mean square (RMS) of ten consecutive readings over 10 s calculated according to Eq. 1.

$$P_{\mathrm{rms}} = \sqrt{\frac{1}{n}\sum_{i=1}^{n}(x_i - \bar{x})^2} \qquad (1)$$

where P_{rms} is the RMS pressure fluctuation or RMS water height (m), n is the number of samples, x_i is the ith pressure sample, and $\bar{x}$ is the mean of the ten pressure samples, giving a measure of variation in depth over time and therefore an indication of water height. The short time period means long-wavelength swell waves are not necessarily measured, but in sheltered coastal areas this is not so important.

The nephelometer readings (nephelometric turbidity units, NTUs) were converted into SSC (mg L^{-1}) using site-specific conversion factors. Sediment collected from the site was resuspended in a container, and after measuring the NTU value of the fine sediment suspension, the sample was filtered through pre-weighed 0.4-μm, 47-mm-diameter polycarbonate filters which were then incubated at 60 °C until constant weight (≥24 h), and the mass determined using a laboratory balance.

Wind speed data (scalar averaged 10 min data in km h^{-1}) to support the field deployment were accessed from the AIMS weather station (S2 Platform, 19°8.460′S, 146°53.390′E) in Cleveland Bay, 10 km NE of the deposition sensor deployment location (Fig. 1).

Results

Measurement principle and sensor calibration

The raw readings (in mV) from the deposition sensor are proportional to how much light is reflected back by sediment that has fallen through the apertures and deposited on the surface of the fibre optic bundles. The relationship between the mV readings and mg cm^{-2} during the calibration process is not always linear as the instrument is less sensitive to the first few particles of sediment until a layer has built up (Figs. 3a, 4). Sediment depositing on the surface of the fibre optics of each of the three sensors is converted to mass (mg) per unit area (cm^2) using the sediment-specific calibrations and the settled amount increases with each 10 min reading until the wiper clears the sediment (every 2 h). The resulting saw-tooth pattern is an indication that net sediment deposition is occurring (Fig. 3b). The sedimentation rate is determined by measuring the slope for each period between wipes and expressed as (mg cm^{-2}, see primary y axis) and can be normalized to a 24-h basis (see secondary y axis) giving a value of mg cm^{-2} d^{-1}. The decrease in the slope over successive 2-h periods occurs because the sediment has progressively settled out of suspension. The inset graph in Fig. 3b shows the cumulative sediment deposition, indicating that >50% of the sediment settled out in the first 2 h of the experiment.

Sedimentation rates are estimated from measurements taken every 10 min over the period between the sensor head wipes. In response to a 50 mg L^{-1} suspension of very fine, light grey carbonate sediment (mean particle size 6.4 ± 0.8 (SE) μm, with 95% of the particles <20 μm), and under static (no flow) conditions, the amount of sediment settling on the surface of the sensor increased with each 10 min reading (Fig. 3b). After 2 h, the fibre optics were automatically wiped clean, returning the sensors to zero and then sediment built up again on the fibre optics over the next 2-h measuring period. This sequence of accumulation and removal results in a 'zigzag' or 'saw-
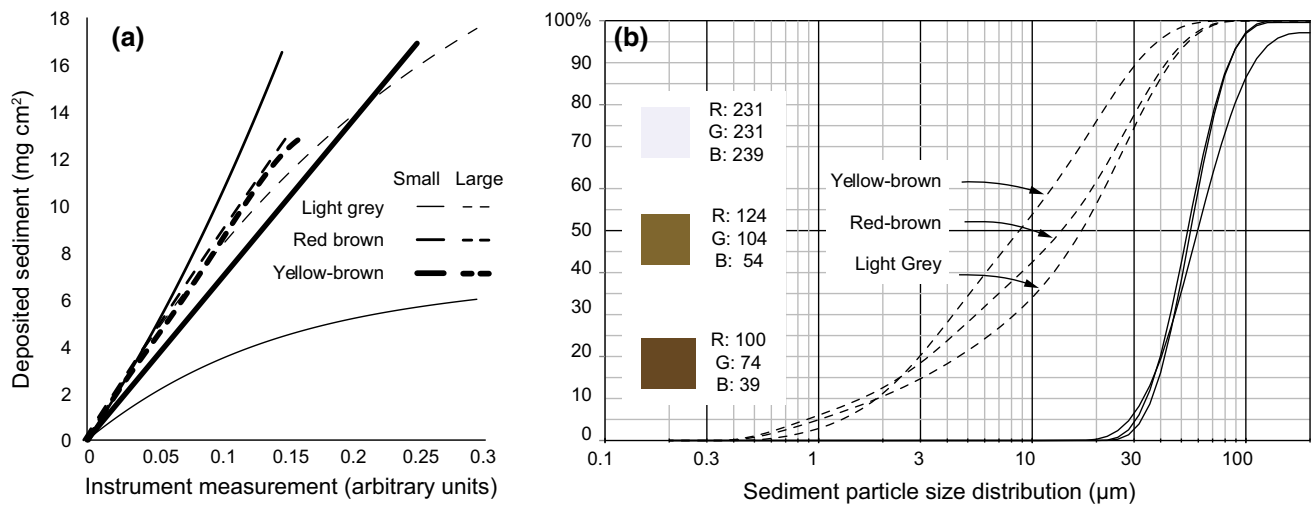
Fig. 4 Sediment calibration for the deposition sensor subjected to sedimentation from **a** three types of sediment each with **b** two different particle size distributions (μm)

tooth' pattern over time (Fig. 3b), indicative of net sediment deposition. The slope of the period between each sensor wipe gives the sedimentation rate, which in Fig. 3b was an average of ∼6 mg cm^{-2} for the first 2-h period, equivalent to ∼72 mg per cm^{-2} d^{-1} if the 2-h rate is converted (normalized) to a 24-h basis. Over the course of the 20-h experiment, there was gradual settlement of the sediment from the water column and the amount of sediment accumulating on the sensor decreased to <0.5 mg cm^{-2} for the last measuring period. The average of all 2-h periods over day was 14.3 mg cm^{-2} d^{-1}, and ∼50% of the sediment settled in the first 2-h measuring period (see Fig. 3b inset), although there was little or no perceptible change in water cloudiness (turbidity) in the tank during this time.

Laboratory tests

The deposition sensor, SedPods and sediment traps gave differing estimates of sediment accumulation [ANCOVA: $F_{(2,86)} = 15.14$; $P < 0.0001$] when exposed to a wide range of different SSC treatments (10–800 mg L^{-1}) under static conditions where sediments dropped out of suspension. A multiple comparison test (TKMC) determined that accumulation values were similar between SedPods and the deposition sensor, while the trap accumulation rate was considerably greater, particularly at high SSCs (Fig. 5).

The experiment was repeated using a 400 mg L^{-1} SSC but under different flow regimes and again sediment deposition varied greatly among instruments [ANCOVA: $F_{(2,35)} = 43.41$; $P < 0.0001$]. Under low flow conditions (2–3 cm s^{-1}), the sediment trap accumulation rate was 40 mg cm^{-2} d^{-1} and 3–4× higher than rates estimated by SedPods and the deposition sensor (range 10–15 mg cm^{-2} d^{-1}; Fig. 6). Under even

higher flow rates (9–17 cm s^{-1}) the sediment trap accumulation rate was >40 mg cm^{-2} d^{-1}, or 4× greater than the accumulation rate estimated by the SedPods (10 mg cm^{-2} d^{-1}) and 15 × higher than the rate estimated by the deposition sensor (2.5 mg cm^{-2} d^{-1}; Fig. 6).

The experiment was repeated using a 400 mg L^{-1} SSC, under high flow rates (9–17 cm s^{-1}) but using different
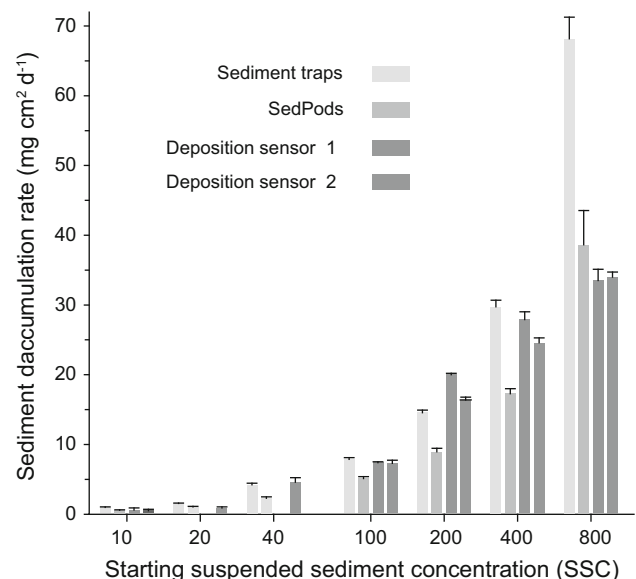

Fig. 5 Sediment accumulation rates estimated by sediment traps (*light grey*), SedPods (*mid-grey*) and deposition sensors (*dark grey*) in response to SSCs over the range 10–800 mg L^{-1}. Experiments were conducted under static (no flow) conditions and sediments were allowed to settle out of suspension resulting in a range of sedimentation rates. Data for sediment traps and SedPods are mean ± SD, $n = 5$, and for the deposition sensor, mean ± SD of the three sensor blocks. Sediments used were *light grey* carbonate sediments with a volume weight mean size of 29 μm
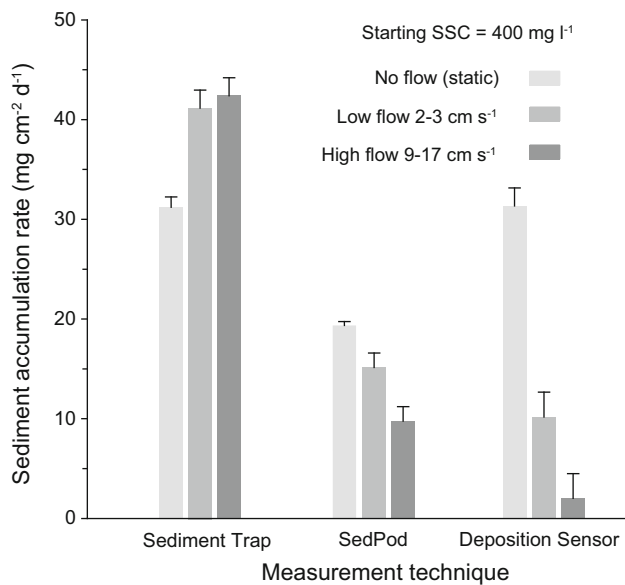
Fig. 6 Sediment accumulation rates estimated by sediment traps, SedPods and deposition sensor in response to a suspended sediment concentration of 400 mg L^{-1}. Experiments were conducted under static (no flow, *light grey*), low flow (*mid-grey*) and higher flow (*dark grey*) conditions. Data for sediment traps and SedPods are mean ± SD, n = 5, and for the deposition sensor the mean ± SD of three sensor blocks. Sediments used were carbonate sediments with a volume weight mean size 29 μm

types and colours of sediments, including very small PSDs with the median particle size by volume (D50) <20 μm. For all three sediment types, deposition rates estimated by the sediment traps (40–60 mg cm^{-2} d^{-1}) were approximately 10× greater than the accumulation rate estimated by the SedPods and deposition sensor (1.5–5 mg cm^{-2} d^{-1}; Fig. 7) [ANCOVA: $F_{(2,33)} = 375.72$; $P < 0.0001$].

Field tests

In the first half of deployment wind speeds were typically low (<20 km h^{-1}), SSCs were <10 mg L^{-1} and sediment deposition rates ranged 4–25 mg cm^{-2} d^{-1}, with an average and median value of 8 and 7 mg cm^{-2} d^{-1}, respectively (Fig. 8). During the second half of the deployment there was a 7-d period and then a 3-d period (referred to as peaks 1 and 2 in Fig. 8), when the average 10 min wind speeds exceeded 30 km h^{-1}, and also exceeded the 95th percentile (P_{95}) and P_{99} of wind speed data collected at the Cleveland Bay weather station S2 since records began in 1999. Associated with these two periods there was an increase in RMS water height (Fig. 8), and SSCs increased from <5 to ∼40–50 mg L^{-1} with short-term peaks over 100 mg L^{-1} (Fig. 8). These high SSCs reduced benthic PAR levels from midday peaks of ∼200–300 μmol quanta m^2 s^{-1} [or a daily light integral (DLI) of 5 mol quanta m^{-2}] to a maximum instantaneous PAR value of <10 μmol quanta m^{-2} s^{-1} and DLIs of 0–0.4 mol quanta m^{-2}. Sediment deposition rates increased from typically <10 mg cm^{-2} d^{-1} before the two peaks in turbidity to a maximum of 53 mg cm^{-2} d^{-1}, decreasing to ∼10 mg cm^{-2} d^{-1} for a few days before the instrument was retrieved (Fig. 8). Average and median deposition rates during the second half of the deployment were 30 and 34 mg cm^{-2} d^{-1}, respectively, or ∼4–5× higher than the first half of the deployment.

A finer-scale analysis of hydrometeorological conditions showed that the high wind event of 3–11 August (peak 1 in Fig. 8) coincided with a transition from neap to spring tides (Fig. 9). Sediment deposition was initially very low (∼5 mg cm^{-2} d^{-1}), but as SSC levels increased the deposition sensor began showing the characteristic saw-
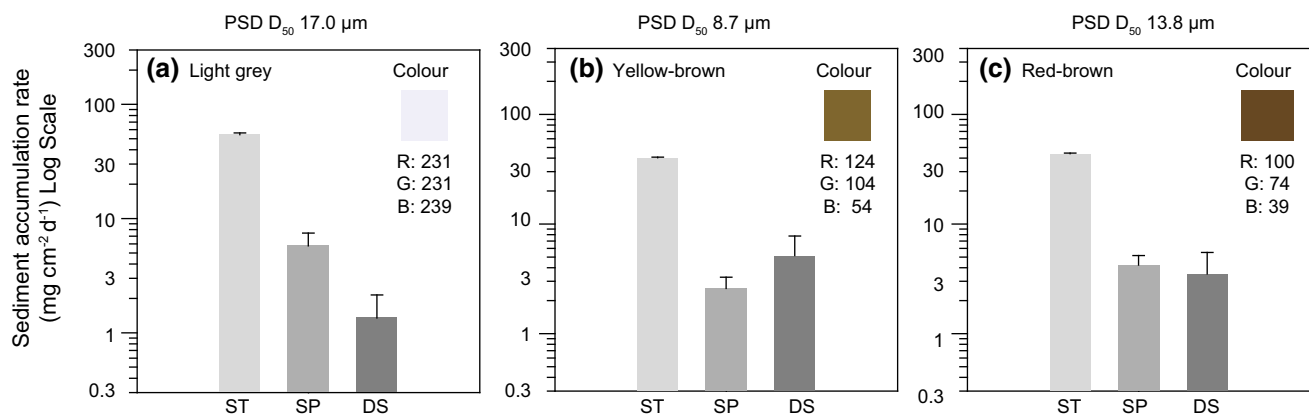

Fig. 7 Sediment accumulation rates estimated by sediment traps (ST), SedPods (SP) and the deposition sensor (DS) exposed to a 400 mg L^{-1} suspension of finely ground sediments: **a** *light grey* calcium carbonate sediment, **b** *yellow-brown* mixed siliciclastic/carbonate sediment, and **c** *red-brown* primarily siliciclastic sediment under flow rates of 9–17 cm s^{-1}. Particle size distributions (PSD) are expressed as the median particle size by volume (D$_{50}$)

Fig. 8 Time series data of hydrometeorological conditions during the deposition sensor deployment at Middle Reef from 14 July to 24 August 2014 showing: **a** water depth (m), **b** underwater photosynthetically active radiation (PAR, μmol photons m^{-2} s^{-1}) and daily light integrals (DLI, mol photons m^{-2} **c** wind speed (km h^{-1}), **d** root mean square (RMS) wave height (m), **e** nephelometrically derived suspended sediment concentration (SSC) (mg l^{-1}) and **f** sediment accumulation rate (mg cm^{-2} d^{-1}). *Dashed line* represents the 95th percentile (P_{95}) and P_{99} of 10-min average wind speed readings recorded at the Cleveland Bay S2 weather station 1999–2015. Peak 1 and peak 2 show two high wind events
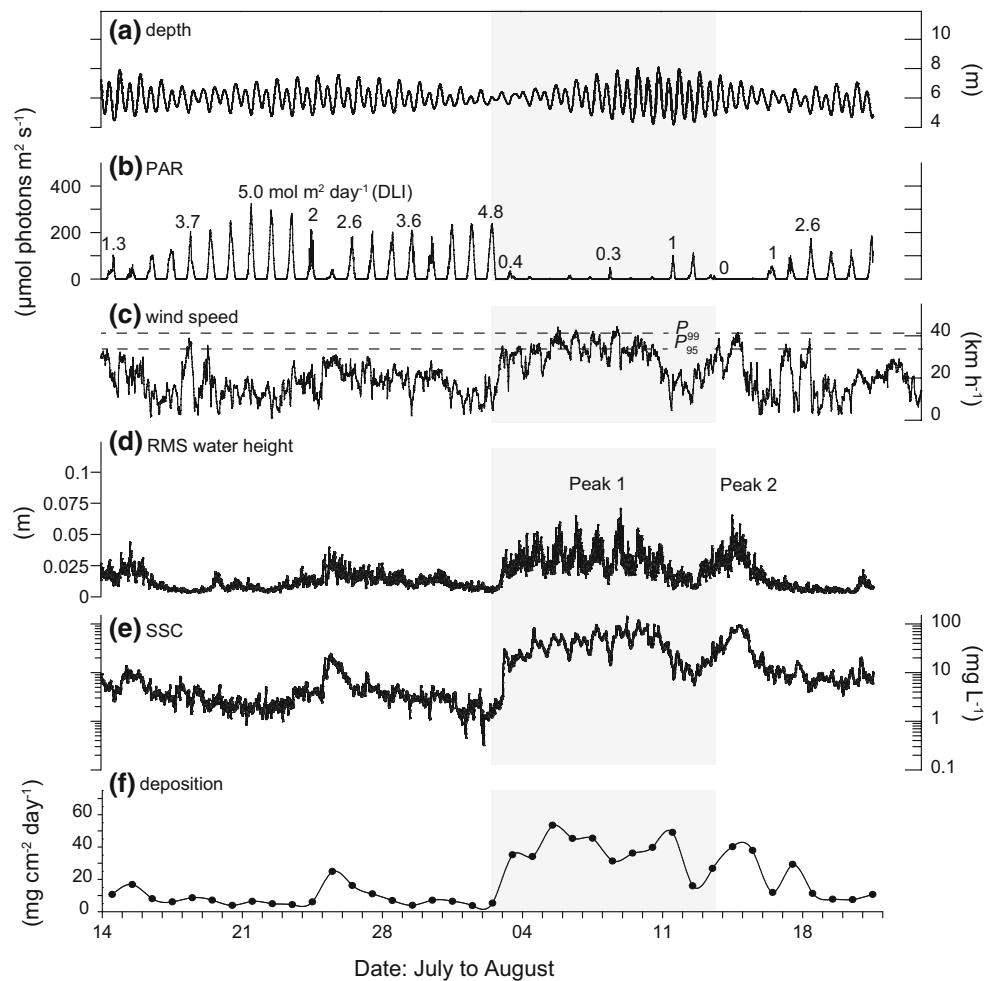
tooth pattern signifying net sediment deposition (Fig. 9 inset). Average daily deposition rates increased $\sim 10\times$, to a maximum of 53 mg cm^{-2} d^{-1}, decreasing to 16 mg cm^{-2} d^{-1} on 12 August as wind speed, RMS water height and SSCs were all decreasing at the end of the high wind event (Fig. 9).

From 7 August, the sub-daily pattern of deposition showed prominent peaks (see grey bands in Fig. 9), where over 1–3-h periods sediment accumulation rate approximately doubled, from 2–3 to 4–6 mg cm^{-2} of sediment per 1-h measuring period. These peaks occurred a few hours after the low tide and initially occurred once a day and at night time (or early morning, Fig. 9). From 9 to 10 August, after the maximum SSCs of >100 mg L^{-1} and when wind speed and RMS water height were decreasing, the peaks occurred twice a day for a few hours after each low tide (Fig. 9).

The average daily sediment deposition rate was 19 $\pm$ 15 mg cm^{-2} d^{-1} (mean $\pm$ SD, $n = 39$ d) over the deployment, and median deposition rate was 11 mg cm^{-2} d^{-1}. Exceedance curves for SSC and sediment deposition are shown together with other percentile values in Fig. 10.

Discussion

The data presented here show previously undescribed sub-daily patterns of sedimentation near a reef in the turbid coastal central GBR, providing new insights into both relative patterns and absolute values of what is considered one of the key pollutants on coral reefs. Earlier versions of the deposition sensor used in this study have been deployed in situ in Japan, Papua New Guinea and the inshore central GBR (Thomas et al. 2003a; Thomas and Ridd 2005). The instruments have since been reconfigured involving a change from a single sensor block and fibre optics combination to a triangular pattern of three sensor blocks each with five bundles of fibre optics. The other design change was more significant and involved a move away from a smooth (glassy) measuring surface to a more topographically complex, rugose, surface that more closely approximates a coral. Choosing a representative surface is difficult because at the macroscale, coral growth form can be highly varied (Pratchett et al. 2015). At the microscale most corals are made up many individual polyps that sit within a

Fig. 9 Fine-scale time series analysis of hydrometeorological conditions during the deposition sensor deployment at Middle Reef during a high wind event in the over the period 2–13 August 2014 showing **a** wind speed (km h^{-1}), **b** nephelometrically derived suspended sediment concentration (SSC) (mg L^{-1}) and root mean square (RMS) wave height (m) and **c** sediment accumulation rate (mg cm^{-2}) and sea level (m). *Horizontal grey boxes* in (**a**) show sea breezes, and *vertical grey boxes* show enhanced sediment deposition events (see text). *Numbers in the grey boxes at the bottom of* (**c**) refer to the average sedimentation rate per day (mg cm^{-2} d^{-1}) derived from the 1 h readings. *Black bars* from 1800 to 0600 h each day signify night time. The *inset* figure shows the saw-tooth pattern for 11 August
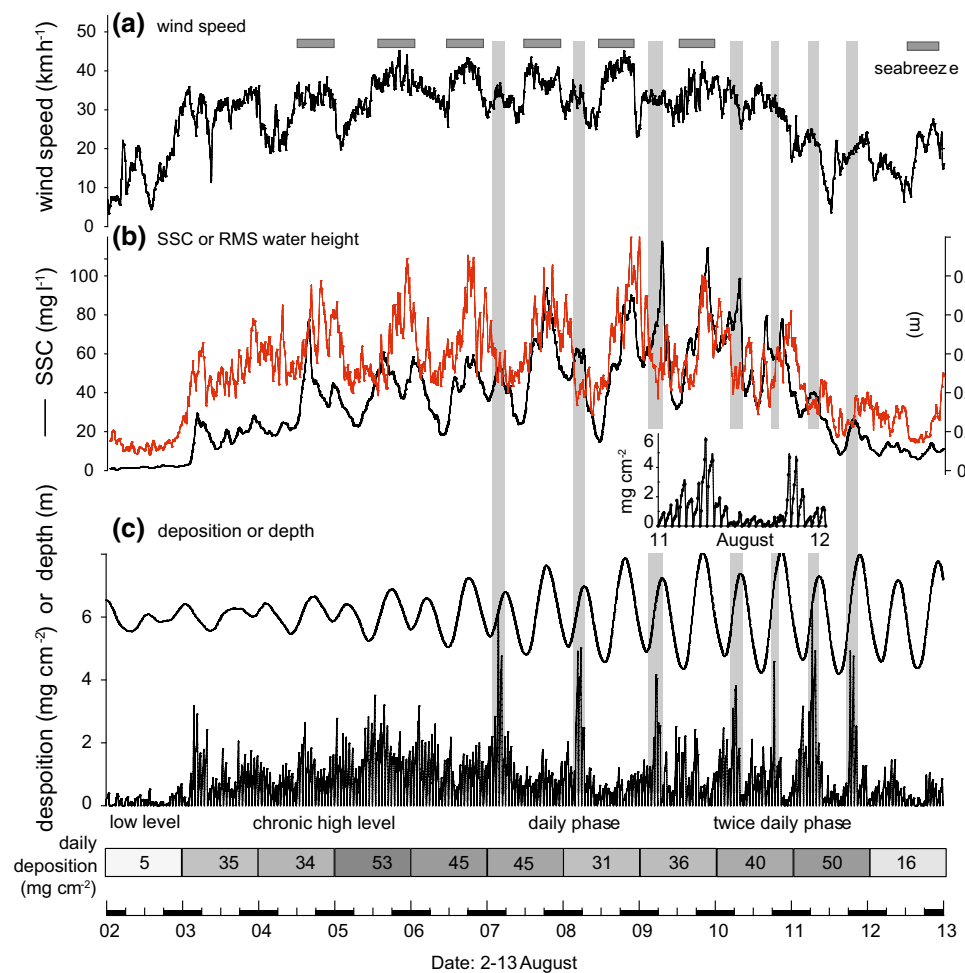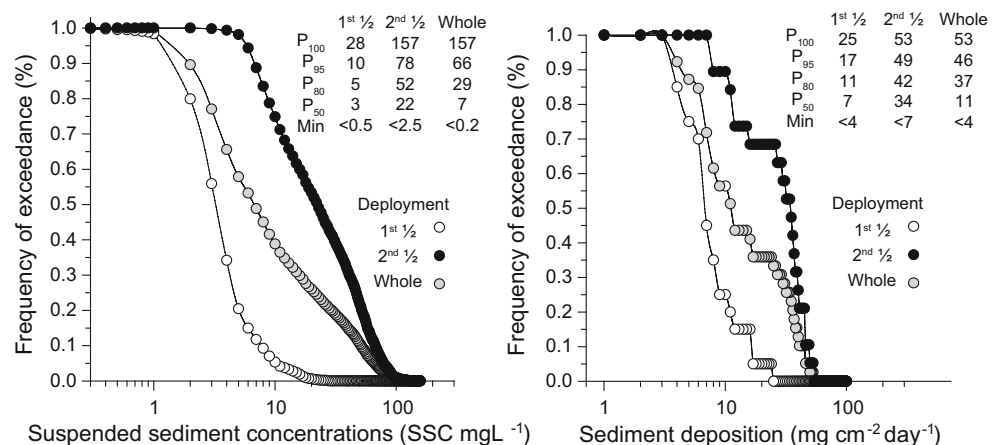

Fig. 10 Nephelomterically derived suspended sediment concentration SSC (mg L^{-1}) and near-bed sediment deposition (mg cm^{-2} d^{-1}) exceedance curves for the deployment at Middle Reef (central, inshore GBR)

skeletal cup or corallite, and the corallites are also highly varied in size, shape and spacing. If they share a wall with neighbouring polyps they are called cerioid, or meandroid if the joining walls form valleys; if the corallites have their own walls they are referred to as plocoid, or phaceloid depending how tall or tubular they are. These combinations of macro (growth form) morphology and micro (corallite size, shape and spacing) morphology result in numerous possible permutations and a multitude of different surface textures and rugosity to choose from. An important practical consideration was also the need for a standardized, uniform and easily reproducible surface; this was more important than modelling a specific coral. The final choice was a horizontal plane with multiple, identical, non-

adjoining and regularly spaced, circular, medium-sized concave depressions representing the corallites. Using coral terminology, the sensor head plate represents a coral with an explanate growth form, medium- to large-sized (6 mm diameter) plocoid-like corallites, with a small inter-corallite (coenosteum) spacing.

The deposition sensor uses the OBS principle which is well known to be sensitive to the number, size, colour, density and shape of suspended particles and refractive index (Conner and De Visser 1992; Gibbs and Wolanski 1992; Thackston and Palermo 2000; Gray and Gartner 2010; Storlazzi et al. 2015). The calibration experiments showed the instrument was reasonably insensitive to sediments of different texture and colour, in part because the PSDs used were quite similar and typical of those in dredging plumes (Jones et al. 2016). The instrument was most sensitive to the light grey sediment from Davies Reef which is probably due to a higher level of reflection of the infra-red, indicating that, as with the use of nephelometers, site-specific calibration is needed depending on the expected type of sediment PSD (see Fig. 4).

The laboratory testing of the deposition sensor against conventional sediment traps and SedPods highlighted some of the well-known issues associated with using sediment traps to estimate deposition in coral reef environments and the difference between gross and net sedimentation. In response to a high concentration of sediment gradually settling under static conditions, the different techniques gave broadly similar results except at very high SSCs. In these experiments, the sediments settled according to Stokes' law and to sediment grain size, density and particle-specific settling velocity. The majority of the sediments settled out during the 24-h experiment, passing through the measuring plane (50 cm below the surface) where the traps, SedPods and deposition sensors were located. Under increasing flow, the deposition sensor and SedPods gave different estimates than sediment traps, and for the deposition sensor the saw-tooth pattern was weak indicating net sedimentation was low. At the highest flow rates tested the accumulation rate estimated by the sensors or by the SedPods was only 2–5 mg cm^{-2} d^{-1}, whereas the traps yielded estimates of 40–50 mg cm^{-2} d^{-1}. Under the flow conditions, the sediments would have been part of turbulent eddies that entered the sediment trap mouth and circulated within the trap body. Beyond a certain depth in the trap, they would have entered a quiescent zone where resuspension forces were insufficient for them to exit, and they became trapped (Storlazzi et al. 2011).

A number of studies have addressed resuspension limitation associated with traps. McClanahan and Obura (1997) note that a factor of three is required to scale up sedimentation rates on flat tiles to those measured with traps. Field et al. (2012) reported that net sediment accumulation on SedPods

was an order of magnitude less than gross accumulation in nearby conventional traps. This is similar to the discrepancy observed in this study. As Storlazzi et al. (2011) noted, in turbulent conditions, sediment traps are much more apt to record information on suspended sediment dynamics than to provide any useful data on sedimentation per se. The implication of these studies is that when sediments from field deployments of traps are dried, weighed, normalized to a surface and expressed as mg cm^{-2} d^{-1}, the result could be an apparent or 'pseudo-sedimentation' rate. Depending on conditions during the deployment, the reported sedimentation rates may partly be an artefact of the trapping process. The deposition sensor has the ability to measure, for the first time, deposition rates on reefs over periods of a few hours as opposed to averages over many days or weeks, and without the resuspension limitation and deposition bias associated with sediment traps.

In situ deployment of the deposition sensor

Measurements were made in Cleveland Bay in the inshore turbid reef zone of the central GBR, which has been the subject of many studies associated with understanding sedimentary processes, sediment transport and fate, and the effects of watershed development on reef growth in marginal, turbid environments (Carter et al. 1993; Larcombe et al. 1995, 2001; Jing and Ridd 1996; Orpin et al. 1999, 2004; Anthony et al. 2004; Browne et al. 2010, 2012, 2013; Lambrechts et al. 2010; Bainbridge et al. 2012; Browne 2012; Orpin and Ridd 2012; Perry et al. 2012; Macdonald et al. 2013; Delandmeter et al. 2015).

Over the course of the deployments, sediment deposition was either barely measureable or occurred in one of two distinct patterns: relatively constant or pulsed. The pulsed pattern was made up of short-term (4–6 h) periods of 'enhanced' deposition which typically began a few hours after low tide, peaking at the mid-tide phase. In the detailed time course shown in Fig. 9, the pulsed deposition occurred in either a diurnal (once a day) or semi-diurnal (twice a day) pattern. Sedimentation rates were similar between modes: ∼42 mg cm^{-2} d^{-1} during 3–6 August (constant mode) or ∼40 mg cm^{-2} d^{-1} during 7–11 August (pulsed mode).

In general terms, SSCs and sedimentation were closely related, in so far as periods of elevated sediment deposition occurred during periods of elevated turbidity. This is intuitive, as resuspended sediment is a prerequisite for sediments to settle out of suspension. The high SSCs were in turn related to elevated wind speeds and wave height, i.e. to wind-wave events. During the study, periods of elevated wind speeds occurred over several days associated with weather fronts and under a diel pattern associated with a locally generated sea breeze. This sea breeze is a prominent feature in Cleveland Bay during the afternoon and early

evening (Larcombe et al. 1995), and the turbidity regime in Cleveland Bay is thought to be determined by high-frequency, short-wavelength wind waves and wave-generated resuspension, in addition to longer wave swell along the GBR which refract into Cleveland Bay (Larcombe et al. 1995; Orpin et al. 1999, 2004).

On a finer, sub-daily timescale the relationship between wind speed, SSCs and sedimentation was uncoupled. Perhaps the most interesting result was the pulsed, enhanced sedimentation events during the deployment that tended to occur when wind speeds were falling associated with the loss of the sea breeze at night time, or a gradual decrease in winds over several days associated with the passing of a weather front. Each of the pulses occurred shortly after a transitory increase in SSCs at the seabed. Our interpretation of these observations is a gradual reduction of near-bed wave-induced orbital velocities related to decreasing wind/waves (associated with loss of the sea breeze at night). However, this cannot account for the transition from the more constant deposition pattern to the pulsed pattern and the transition (and eventual loss) of the diurnal then semi-diurnal pulsed patterns (Fig. 9). These patterns developed following the progression from neap tides (lower tidal range) to spring tides (higher tidal range), and each event occurred after low water, peaking at the mid-tide mark. This suggests tidal modulation of the deposition cycle that could be caused by (1) reduced tidal flows and a settling lag, such that sediments in the water column need time to settle out of suspension onto the sensor, or (2) gradually increasing water depth at the mid-tide point, reducing wave orbital velocities and enhancing settling. An alternative suggestion is that the patterns represent advection of turbid water from Cleveland Bay across the sensors. Without measurements of current speed and direction, it is not possible to consider this further.

The deposition sensor was deployed in a naturally very turbid area over a period of time where SSCs ranged from <1 to as high as 157 mg L^{-1}, and averaged 17 mg L^{-1} (median 7 mg L^{-1}). The exposure period included several spring–neap tidal cycles and a range of wind conditions from calm to extreme. This provided an ideal spectrum of conditions to allow generalizations on the absolute levels of sediment deposition and patterns of deposition in a naturally highly turbid reef environment. For the whole deployment, which included several very high wind events and SSCs >100 mg L^{-1}, deposition rates averaged 19 ± 16 mg cm^{-2} d^{-1} (median deposition rate = 11 mg cm^{-2} d^{-1}). For the first half of the deployment, where SSCs varied from <1 to 28 mg L^{-1}, which are typical for the Cleveland Bay area (Larcombe et al. 1995; Orpin et al. 2004; Macdonald et al. 2013), the deposition rates averaged only 8 ± 5 mg cm^{-2} d^{-1}. This value is very similar to net deposition rates of 3–7 mg cm^{-2} d^{-1}

measured over the course of a year at the same site using shallow trays, which also do not limit sediment resuspension (Browne et al. 2012). These values, especially the upper values, are much lower than sediment trap accumulation rates measured around Magnetic Island and Cleveland Bay which have been reported to range 30–120 mg cm^{-2} d^{-1} (averaging 80 mg cm^{-2} d^{-1}; McIntyre and Associates Pty. Ltd. 1986), 25–243 mg cm^{-2} d^{-1} (averaging 75 mg cm^{-2} d^{-1}, including 27–62 mg cm^{-2} d^{-1} at Middle Reef; Larcombe et al. 1994) and 3–360 mg cm^{-2} d^{-1} (averaging ~50 mg cm^{-2} d^{-1}; Mapstone et al. 1992). As discussed in Jones et al. (2016), in laboratory-based studies of the effects of sedimentation on corals the application rates used, which are based on sediment trap data, are often in the high tens of mg cm^{-2} d^{-1}, commonly hundreds of mg cm^{-2} d^{-1}, and even g cm^{-2} d^{-1}. These application rates have well-described effects on coral physiology, but if based on a measurement technique (sediment traps) which is overestimating sedimentation rates by up to an order of magnitude, the relevance of these application rates needs to be considered, and application of the knowledge to coral reef processes should be cautious (Storlazzi et al. 2011).

The deposition sensor can be constructed from off-the-shelf electronics (LED lights and sensors, fibre optic bundles, servo, data logger and batteries), with some machining required for the sensor head, sensor block and PVC pipe housing. For the many reasons outlined in Field et al. (2012), SedPods offer a viable low-cost coral proxy for measuring net sedimentation, but they do not have self-cleaning mechanisms to prevent biofouling and this precludes extended in situ deployments. Estimates of net sedimentation at a timescale of 24 h by SedPods requires daily boating and diving operations (for collection and redeployment) which comes with logistical and financial costs and safety issues (Llewellyn and Bainbridge 2015). Obvious future directions include extending the deposition sensor deployments to less marginal environments, and quantifying the intensity, duration and frequency of sedimentation events under natural and under anthropogenic influences (such as during dredging campaigns), to define the range of sedimentation rates corals are likely to experience.

References

Anthony K, Connolly S (2004) Environmental limits to growth: physiological niche boundaries of corals along turbidity–light gradients. Oecologia 141:373–384

Anthony K, Ridd P, Orpin A, Larcombe P, Lough J (2004) Temporal variation of light availability in coastal benthic habitats: effects of clouds, turbidity, and tides. Limnol Oceanogr 49:2201–2211

Bainbridge ZT, Wolanski E, Alvarez-Romero JG, Lewis SE, Brodie JE (2012) Fine sediment and nutrient dynamics related to particle size and floc formation in a Burdekin River flood plume, Australia. Mar Pollut Bull 65:236–248

Baker E, Lavelle J (1984) The effect of particle size on the light attenuation coefficient of natural suspensions. J Geophys Res Oceans 89:8197–8203

Bothner MH, Reynolds RL, Casso MA, Storlazzi CD, Field ME (2006) Quantity, composition, and source of sediment collected in sediment traps along the fringing coral reef off Molokai, Hawaii. Mar Pollut Bull 52:1034–1047

Browne NK (2012) Spatial and temporal variations in coral growth on an inshore turbid reef subjected to multiple disturbances. Mar Environ Res 77:71–83

Browne NK, Smithers SG, Perry CT (2010) Geomorphology and community structure of Middle Reef, central Great Barrier Reef, Australia: an inner-shelf turbid zone reef subject to episodic mortality events. Coral Reefs 29:683–689

Browne NK, Smithers SG, Perry CT (2013) Spatial and temporal variations in turbidity on two inshore turbid reefs on the Great Barrier Reef, Australia. Coral Reefs 32:195–210

Browne NK, Smithers SG, Perry CT, Ridd PV (2012) A field-based technique for measuring sediment flux on coral reefs: application to turbid reefs on the Great Barrier Reef. J Coast Res 284:1247–1262

Buesseler KO, Antia AN, Chen M, Fowler SW, Gardner WD, Gustafsson O, Harada K, Michaels AF, der Loeff MR, Sarin M (2007) An assessment of the use of sediment traps for estimating upper ocean particle fluxes. J Mar Res 65:345–416

Butman CA, Grant WD, Stolzenbach KD (1986) Predictions of sediment trap biases in turbulent flows: a theoretical analysis based on observations from the literature. J Mar Res 44:601–644

Carter R, Johnson D, Hooper K (1993) Episodic post-glacial sea-level rise and the sedimentary evolution of a tropical continental embayment (Cleveland Bay, Great Barrier Reef shelf, Australia). Australian Journal of Earth Sciences 40:229–255

Conner CS, De Visser AM (1992) A laboratory investigation of particle size effects on an optical backscatterance sensor. Mar Geol 108:151–159

Cortes JN, Risk MJ (1985) A reef under siltation stress: Cahuita, Costa Rica. Bull Mar Sci 36:339–356

Delandmeter P, Lewis S, Lambrechts J, Deleersnijder E, Legat V, Wolanski E (2015) The transport and fate of riverine fine sediment exported to a semi-open system. Estuar Coast Shelf Sci 167:336–346

English S, Baker V, Wilkinson C (1997) Survey manual for tropical marine resources: Australian Institute of Marine Science Townsville

Erftemeijer PL, Lewis RR (2006) Environmental impacts of dredging on seagrasses: a review. Mar Pollut Bull 52:1553–1572

Field ME, Chezar H, Storlazzi CD (2012) SedPods: a low-cost coral proxy for measuring net sedimentation. Coral Reefs 32:155–159

Foster T, Corcoran E, Erftemeijer P, Fletcher C, Peirs K, Dolmans C, Smith A, Yamamoto H, Jury M (2010) Dredging and port construction around coral reefs. Report No 108, PIANC Environmental Commission, Brussels, Belgium

Gibbs RJ, Wolanski E (1992) The effect of flocs on optical backscattering measurements of suspended material concentration. Mar Geol 107:289–291

Gray JR, Gartner JW (2009) Technological advances in suspended-sediment surrogate monitoring. Water Resour Res 45:1–20

Gray J, Gartner J (2010) Overview of selected surrogate technologies for high-temporal resolution suspended sediment monitoring. Proceedings of the 2nd Joint Federal Interagency Conference (June 27–July 1) Las Vegas, NV, USA, 207 pp

Hargrave BT, Burns NM (1979) Assessment of sediment trap collection efficiency. Limnol Oceanogr 24:1124–1136

ISRS (2004) The effects of terrestrial runoff of sediments, nutrients and other pollutants on coral reefs. Briefing Paper 3, International Society for Reef Studies, 18 pp

Jing L, Ridd PV (1996) Wave-current bottom shear stresses and sediment resuspension in Cleveland Bay, Australia. Coastal Engineering 29:169–186

Jones R, Bessell-Browne P, Fisher R, Klonowski W, Slivkoff M (2016) Assessing the impacts of sediments from dredging on corals. Mar Pollut Bull 102:9–29

Jürg B (1996) Towards a new generation of sediment traps and a better measurement/understanding of settling particle flux in lakes and oceans: a hydrodynamical protocol. Aquat Sci 58:283–296

Kozerski H-P (1994) Possibilities and limitations of sediment traps to measure sedimentation and resuspension. Hydrobiologia 284:93–100

Lambrechts J, Humphrey C, McKinna L, Gourge O, Fabricius KE, Mehta AJ, Lewis S, Wolanski E (2010) Importance of wave-induced bed liquefaction in the fine sediment budget of Cleveland Bay, Great Barrier Reef. Estuar Coast Shelf Sci 89:154–162

Larcombe P, Costen A, Woolfe KJ (2001) The hydrodynamic and sedimentary setting of nearshore coral reefs, central Great Barrier Reef shelf, Australia: Paluma Shoals, a case study. Sedimentology 48:811–835

Larcombe P, Ridd PV, Wilson B, Prytz A (1994) Sediment data collection. In: Benson LJ, Goldsworthy PM, Butler IR, Oliver J (eds) Townsville Port Authority Capital Dredging Works 1993. Environmental Monitoring Program. Townsville Port Authority, Townsville, Queensland, Australia, pp 149–163

Larcombe P, Ridd P, Prytza A, Wilson B (1995) Factors controlling suspended sediment on inner-shelf coral reefs, Townsville, Australia. Coral Reefs 14:163–171

Llewellyn LE, Bainbridge SJ (2015) Getting up close and personal: the need to immerse autonomous vehicles in coral reefs. OCEANS 2015-MTS/IEEE Washington, 19–22 October 2015, pp 1–9

Macdonald RK, Ridd PV, Whinney JC, Larcombe P, Neil DT (2013) Towards environmental management of water turbidity within open coastal waters of the Great Barrier Reef. Mar Pollut Bull 74:82–94

Mapstone BD, Choat J, Cumming R, Oxley W (1992) The fringing reefs of Magnetic Island: benthic biota and sedimentation-a baseline study. Research report No. 13, Great Barrier Reef Marine Park Authority, Townsville, Australia

McClanahan T, Obura D (1997) Sedimentation effects on shallow coral communities in Kenya. J Exp Mar Bio Ecol 209:103–122

McIntyre and Associates Pty. Ltd. (1986) Magnetic Keys Development, Nelly Bay, Magnetic Island. Impact Assessment Study, May 1986

Ogston AS, Storlazzi CD, Field ME, Presto MK (2004) Sediment resuspension and transport patterns on a fringing reef flat, Molokai, Hawaii. Coral Reefs 23:559–569

Orpin AR, Ridd PV (2012) Exposure of inshore corals to suspended sediments due to wave-resuspension and river plumes in the central Great Barrier Reef: a reappraisal. Cont Shelf Res 47:55–67

Orpin A, Ridd P, Stewart L (1999) Assessment of the relative importance of major sediment transport mechanisms in the central Great Barrier Reef lagoon. Australian Journal of Earth Sciences 46:883–896

Orpin A, Ridd P, Thomas S, Anthony K, Marshall P, Oliver J (2004) Natural turbidity variability and weather forecasts in risk management of anthropogenic sediment discharge near sensitive environments. Mar Pollut Bull 49:602–612

Perry CT, Smithers SG, Gulliver P, Browne NK (2012) Evidence of very rapid reef accretion and reef growth under high turbidity and terrigenous sedimentation. Geology 40:719–722

Pratchett M, Anderson K, Hoogenboom M, Widman E, Baird A, Pandolfi J, Edmunds P (2015) Spatial, temporal and taxonomic variation in coral growth—implications for the structure and function of coral reef ecosystems. Oceanogr Mar Biol Annu Rev 53:215–295

Reynolds CS, Wiseman SW, Gardner W (1980) An annotated bibliography of aquatic sediment traps and trapping methods. Occasional Publication No. 11, Freshwater Biological Association, UK, 54 pp

Ridd P, Day G, Thomas S, Harradence J, Fox D, Bunt J, Renagi O, Jago C (2001) Measurement of sediment deposition rates using an optical backscatter sensor. Estuar Coast Shelf Sci 52:155–163

Risk MJ, Edinger E (2011) Impacts of sediment on coral reefs. In: Hopley D (ed) Encyclopedia of modern coral reefs. Springer, Netherlands, pp 575–586

Rogers CS (1990) Responses of coral reefs and reef organisms to sedimentation. Mar Ecol Prog Ser 62:185–202

Storlazzi CD, Field ME, Bothner MH (2011) The use (and misuse) of sediment traps in coral reef environments: theory, observations, and suggested protocols. Coral Reefs 30:23–38

Storlazzi C, Norris B, Rosenberger K (2015) The influence of grain size, grain color, and suspended-sediment concentration on light attenuation: why fine-grained terrestrial sediment is bad for coral reef ecosystems. Coral Reefs 34:967–975

Thackston E, Palermo MR (2000) Improved methods for correlating turbidity and suspended solids for monitoring. US Army Engineer Research and Development Center, Vicksberg, MS, p 12

Thomas S, Ridd PV (2004) Review of methods to measure short time scale sediment accumulation. Mar Geol 207:95–114

Thomas S, Ridd P (2005) Field assessment of innovative sensor for monitoring of sediment accumulation at inshore coral reefs. Mar Pollut Bull 51:470–480

Thomas S, Ridd PV, Day G (2003a) Turbidity regimes over fringing coral reefs near a mining site at Lihir Island, Papua New Guinea. Mar Pollut Bull 46:1006–1014

Thomas S, Ridd PV, Renagi O (2003b) Laboratory investigation on the effect of particle size, water flow and bottom surface roughness upon the response of an upward-pointing optical backscatter sensor to sediment accumulation. Cont Shelf Res 23:1545–1557

Wolanski E (1994) Physical oceanographic processes of the Great Barrier Reef. CRC Press, Boca Raton, FL